Jpn. J. Appl. Phys. Vol. 39 (2000) pp. L 958–L 960
Part 2, No. 10A, 1 October 2000

Local Stress Analysis of Epitaxial Laterally-Overgrown GaN

Quincy LIU*, Axel HOFFMANN[1], Axel KASCHNER[1], Christian THOMSEN[1], Jürgen CHRISTEN[2], Peter VEIT[2] and Rainer CLOS[2]

Abteilung Theoretische Physik, Hahn-Meitner-Institut, Glienicker Str. 100, D-14109 Berlin, Germany
[1]*Institut für Festkörperphysik, Technische Universität, D-10623 Berlin, Germany*
[2]*Institut für Experimentelle Physik, Otto-von-Guericke-Universität Magdeburg, D-39016 Magdeburg, Germany*

(Received May 16, 2000; accepted for publication August 18, 2000)

Three-dimensional stress distributions for two different samples of epitaxial laterally-overgrown GaN deposited on SiO_2 masks were simulated by continuum elasticity theory using the finite-element method. The samples have patterned masks in the $(1\bar{1}00)$ and $(11\bar{2}0)$ orientations, respectively. The results of the simulation compared quantitatively quite well with the stress distributions derived from micro-Raman measurements. This success depended on taking into account the existence of a string of voids in the samples that could be seen in the transmission electron microscope image. From the buffer layer towards the sample surface, the biaxial stress relaxes within a relatively short distance to a value that corresponds to a biaxially compressed film. This value persists until a short distance from the sample surface.

KEYWORDS: epitaxial laterally-overgrown GaN, micro-Raman, transmission electron microscopy, strain relaxation, finite-elements analysis

1. Introduction

In the pursuit of high quality GaN that has superior optical and electrical properties, the epitaxial lateral overgrowth (ELOG) technique[1)] has been shown to be effective in reducing the dislocation density in GaN on sapphire substrates.[2)] Going beyond the basic optical characterization,[3,4)] two recent works[5,6)] have reported comprehensive microscopic characterization of near band gap emission by spectrally resolved cathodoluminesence (CL) spectroscopy and micro-Raman (μ-Raman) spectroscopy, correlating the local optical and structural properties of the ELOG GaN structures.

In support of the experimental characterization,[5,6)] we present in this work stress distributions obtained from simulation based on continuum elasticity theory using the three dimensional finite-element method (FEM).[7)] We compare the theoretical results with the stress distributions derived from μ-Raman spectroscopy, and thereby obtained an interpretation of the experimental data that is consistent with previous findings in the literature. Details of the experimental technique and set-up of the μ-Raman spectroscopy can be found in refs. 5 and 6.

2. Experimental Data

Each of the two samples under discussion consists of a 3 μm thick GaN buffer layer grown by metalorganic vapor phase epitaxy (MOVPE) on (0001) sapphire and covered with a 120 nm thick patterned SiO_2 mask. The pattern is made up of alternate parallel stripes of mask material and openings that have identical widths of 10 μm. In one sample the stripes are oriented along the $\langle 11\bar{2}0\rangle$ direction (the $\langle 11\bar{2}0\rangle$ sample),[5)] while in the other along $\langle 1\bar{1}00\rangle$ (the $\langle 1\bar{1}00\rangle$ sample).[6)] Further deposition of GaN by hydride vapor phase epitaxy (HVPE) led to the growth of GaN through the openings or windows in the mask and the lateral overgrowth above the SiO_2 stripes. The maximum heights of the second deposition are around 42 μm and 50 μm for the $\langle 11\bar{2}0\rangle$ and $\langle 1\bar{1}00\rangle$ samples, respectively. Images of the samples from scanning electron microscope (SEM) can be found in refs. 5 and 6.

In Fig. 1, we show a transmission electron microscope (TEM) image of the $\langle 11\bar{2}0\rangle$ ELOG sample, directly above the midpoint of the SiO_2 stripe of the mask. Clearly discernable is a string of voids that runs uninterrupted from the SiO_2 stripe to the ELOG surface. It seems that the ELOG does not fuse together as GaN is grown laterally over the stripe. Similar voids are found in the $\langle 1\bar{1}00\rangle$ sample.

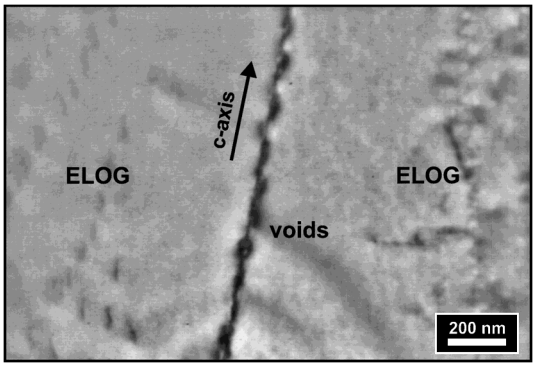

Fig. 1. TEM image of the voids observed in the coalescence region of the $\langle 11\bar{2}0\rangle$ sample of GaN ELOG. A similar image is observed for the $\langle 1\bar{1}00\rangle$ sample.

For each of the samples, μ-Raman measurements were made along two loci that run in the $\langle 0001\rangle$ direction from the buffer to the top surface of the ELOG-one through the midpoint of the window and the other through the midpoint of the SiO_2 stripe. The Raman shift of the E_2 (high) phonon mode can be parametrized[8)] in terms of the biaxial stress σ_{xx}. The plots of the values of σ_{xx} along the loci can be found in Fig. 3 of ref. 5 and Fig. 4 of ref. 6.

3. Results and Discussion

Using FEM to simulate stress distribution has become a common and useful tool in the study of semiconductor heterostructures. Some details of its application can be found in, for example, ref. 9. Our previous success in the stress analysis of GaN selective epitaxial overgrowth[10)] has encouraged us to adopt the same strategy in our present FEM simulations. Namely, we use a set of moduli of elasticity for GaN found in the literature[10,11)] and an effective mismatch α_{eff} between the sapphire substrate and the GaN buffer above it. α_{eff} is

*E-mail address: liu@hmi.de

parametrized to account for the defects, impurities, and dislocations in the GaN. Specifically, α_{eff} was adjusted to reproduce the biaxial stress σ_{xx} in the buffer. We shall discuss the values of α_{eff} for the two samples in a later paragraph. However, one ought to be aware that in the ELOG there is a significant spatial variation of crystalline quality. This might lead to further spatial adjustment of α_{eff}.

For clarity in discussion, we shall designate the GaN that has grown above the window as the 'window GaN' and above the SiO_2 stripe as the 'mask GaN'.

We display in Fig. 2 the unit cells of our FEM simulation. In Fig. 2(a), the unit cell describes the case of the $\langle 11\bar{2}0\rangle$ sample.[5] The width MW of the cell is 10 μm in the $\langle 1\bar{1}00\rangle$ direction, and the depth is 4 μm in the $\langle 11\bar{2}0\rangle$ direction. Extended from the left for 5 μm and at a height of 3 μm is the SiO_2 mask material of thickness 120 nm. We impose periodic boundary conditions at the side planes that are perpendicular to the $\langle 1\bar{1}00\rangle$ and $\langle 11\bar{2}0\rangle$ directions. The line M′W′ is on the $\langle 1\bar{1}01\rangle$ facet seen in the SEM picture. The lines WW′ and MM′ are the window and mask loci along which μ-Raman measurements have been made. In Fig. 2(b) we show the unit cell for the $\langle 1\bar{1}00\rangle$ sample.[6] In place of the $\langle 1\bar{1}01\rangle$ facet on the ELOG surface, there is only a small indentation directly above the middle of the stripe.

The string of voids mentioned previously are dotted along MM′. These voids can be as wide as 50 nm and continue all the way to the surface of the ELOG. It is unrealistic to expect that we could construct, for the simulations, the actual shapes and sizes of the voids down to the distribution of atoms surrounding them. Moreover, the shapes and sizes (around a certain spatial dimension of 50 nm) of these voids must have a high degree of randomness. Hence, for simplicity we have used a schematic representation of the shape and a spatial dimension of approximately 50 nm, and their configurations are shown in Fig. 2(c).

The biaxial stresses σ_{xx} in the buffer of the $\langle 11\bar{2}0\rangle$ and $\langle 1\bar{1}00\rangle$ samples have been observed to be ≈ -0.5 GPa and ≈ -0.8 GPa, respectively.[5,6] In the FEM simulations we have therefore used two different effective mismatches α_{eff} in order to reproduce the σ_{xx} in the buffers correctly, and they are -0.15% and -0.11%, respectively. In the respective cases, we assign the same effective mismatch to the window GaN. For the mask GaN, it seems reasonable to assign a different effective mismatch α_{eff} since a reduction of three to four orders of magnitude in threading dislocation densities has been observed.[2] For the present report we have used $\alpha_{\text{eff}} = 0$ for the mask GaN in both samples. The value implies that there is no mismatch between the mask GaN and the SiO_2 stripe of the mask. The justification of the idea is that the SiO_2 that makes up the mask is amorphous which allows the mask GaN to slide relatively unrestrained over its surface. A more refine model to describe the contact and friction between the crystalline GaN and amorphous SiO_2 might be warranted in the future.

We have summarized the results for σ_{xx} along the designated loci in the two samples in Fig. 3. In view of our self-imposed limited variation of parameters, the agreement between the simulations and the experimentally derived values is quite good. One salient feature stands out from Fig. 3 is that the biaxial stress σ_{xx} has the characteristics of that of a film, albeit of thickness of μm. For example, for the window loci WW′ of both samples, σ_{xx} relaxes rapidly through the window to values of -0.32 GPa, in Fig. 3(a), and -0.45 GPa, in Fig. 3(c), respectively. For the $\langle 11\bar{2}0\rangle$ sample of Fig. 3(a), this value remains approximately constant until the height of ≈ 23 μm is reached where the $\langle 1\bar{1}01\rangle$ facet begins to develop on the other side of the unit cell. Beyond 23 μm σ_{xx} relaxes further because the open $\langle 1\bar{1}01\rangle$ facet facilitates the relaxation in the x-y direction. For the $\langle 1\bar{1}00\rangle$ sample of Fig. 3(c), σ_{xx} throughout the window region is mostly ≈ -0.45 GPa, until one approaches the ELOG surface where a further relaxation occurs. This latter is caused by the small indentation on the other side of the unit cell. This constant in value for σ_{xx} is a characteristic of a biaxially compressed film.

The values for σ_{xx} along the mask loci MM′ of both samples are summarized in Figs. 3(b) and 3(d). They also exhibit the characteristics of values from a biaxially stressed film. By construction the loci MM′ are slightly displaced from the exact midpoint of the stripe because of the existence of the string of voids.

We have found in the simulations that the existence of the voids plays an important and subtle role in determining the quality of the agreement between the simulation and the experiment. Without the explicit introduction of voids in the

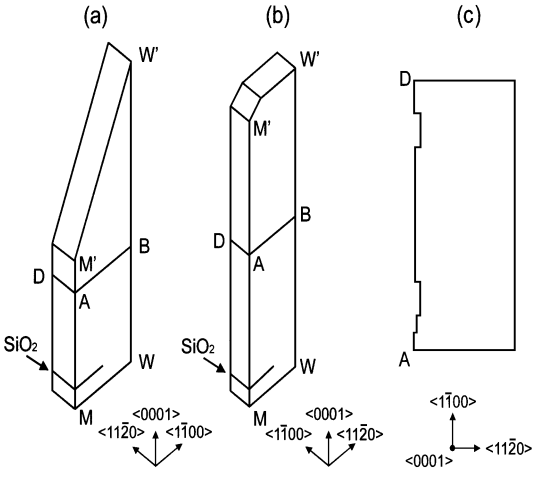

Fig. 2. (a) FEM unit cell of the $\langle 11\bar{2}0\rangle$ sample; (b) FEM unit cell of the $\langle 1\bar{1}00\rangle$ sample; (c) schematic form of the voids used in the FEM.

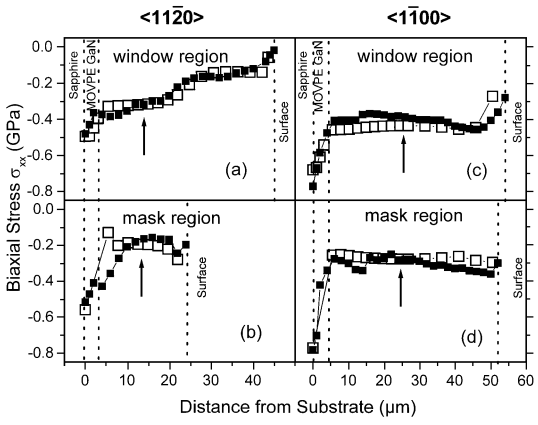

Fig. 3. Comparison of theoretical (white boxes) and experimentally derived (black boxes) biaxial stresses σ_{xx} along the window loci WW′ and mask loci MM′ in the samples. The arrows indicate the positions of the cross sectional area ABCD of Figs. 2 and 4.

simulation, it was quite difficult to obtain agreements along the loci WW′ and MM′ simultaneously unless further spatial variations of the effective mismatch α_{eff} were included. Furthermore, the absolute values of α_{eff} would have been of a different order of magnitude, rendering our present simulation inconsistent with our previous findings.[10] Apparently, the possibility of full relaxation around the voids affects σ_{xx} in the window region that is some distance away from them.

On the other hand, neither the present μ-Raman measurements nor the σ_{xx} from simulation, to a large extent, depends on the detailed shape of the voids. It is important to remember that to expose the $(11\bar{2}0)$ and $(1\bar{1}00)$ planes by cracking so that μ-Raman spectroscopy could be carried out, the sizes and shapes of the voids that were made visible could not be predicted. This implies a certain unpredictability for the measured biaxial stress σ_{xx} in the surrounding of the voids. However, the variation of σ_{xx} in the general spatial dimension of of the voids, i.e., in nm, is smoothened out within the spatial resolution of the μ-Raman spectroscopy of 0.7 μm.

To examine the influence of the shape of the voids on our simulation results, we show in Fig. 4 the stress σ_{xx} in a cross-sectional area ABCD of our unit cells. The positions of ABCD in the two samples are indicated in Figs. 2 and 3. For the $\langle 11\bar{2}0\rangle$ sample, Fig. 4(a), this cross-sectional area is 14 μm above the mask, and for the $\langle 1\bar{1}00\rangle$ sample, Fig. 4(b), it is 24 μm. From inspection of Fig. 3, these heights correspond to locations where the simulations predict that σ_{xx} has the characteristics of a biaxially compressed film as discussed in the previous paragraphs. The notable features of σ_{xx} in Fig. 4 are that away from the voids, the values picked out by the loci WW′ and MM′ can be found over a large area surrounding our loci. For example, in Fig. 3(c), WW′ picks out the value $\sigma_{xx} \approx -0.45$ GPa at 24 μm. We see in Fig. 4(b) that this value of σ_{xx} can be found over a large area on the right half of the figure, in particularly, close to the line BC. Similarly, one finds $\sigma_{xx} \approx -0.28$ GPa over a large area on the left half of the figure. Approximately the *same* distribution

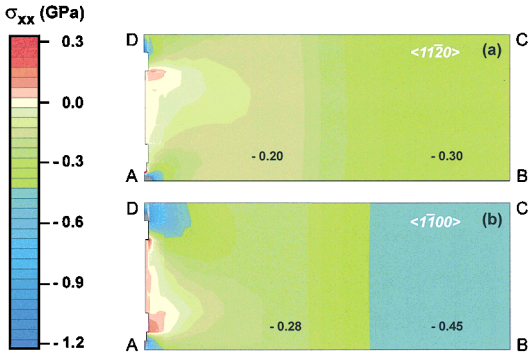

Fig. 4. Theoretical biaxial stress σ_{xx} on the cross-sectional surface ABCD in the samples.

of σ_{xx} could be obtained when we used *different* schematic representation of the voids. These results are indications to us that the results from simulation, as summarized in Fig. 3, are independent of (1) how the samples were cracked to expose the $\langle 11\bar{2}0\rangle$ and $\langle 1\bar{1}00\rangle$ planes and (2) the detail of the shapes of the voids.

4. Conclusion

In conclusion, the FEM study of the biaxial stresses of the GaN ELOG samples has led us to interpret the experimental μ-Raman data to have the characteristics of a biaxially compressed film. Close to the surface of the samples, the stress distributions depend on the surface roughness. The absolute values of the biaxial stresses inside the ELOG depend on the mismatch to the substrate and the local spatial concentrations of impurities, dopants, and density of threading dislocation. In the FEM simulations these are parametrically represented by the effective mismatch α_{eff}. We could simulate the results from the experiment by choosing a suitable value for α_{eff}, provided the existence of the voids in the ELOG is reasonably represented. The importants lesson learned from our results are twofold. (1) That this suitable value of α_{eff} is consistent with our previous findings[10] strengthens our interpretation of the μ-Raman data. In contrast, if the agreement with the data is achieved at the expense of arbitrary variations of numerous parameters, then any interpretation might have been meaningless. (2) Since ELOG results from growth through masks, voids in the ELOG above the masks are unavoidable. We have demonstrated that any theoretical study of the stress distributions must take them into consideration.

1) Y. Kato, S. Kitamura, K. Hiramatsu and N. Sawaki: J. Cryst. Growth **144** (1994) 133.
2) A. Usui, H. Sunakawa, A. Sakai and A. Yamaguchi: Jpn. J. Appl. Phys. **36** (1997) L899.
3) J. A. Freitas, O.-H. Nam, R. F. Davis, G. V. Saparin and S. K. Obyden: Appl. Phys. Lett. **72** (1998) 2990.
4) X. Li, S. G. Bishop and J. J. Coleman: Appl. Phys. Lett. **73** (1998) 1179.
5) F. Bertram, T. Riemann, J. Christen, A. Kaschner, A. Hoffmann, C. Thomsen, K. Hiramatsu, T. Shibata and N. Sawaki: Appl. Phys. Lett. **74** (1999) 359.
6) A. Kaschner, A. Hoffmann, C. Thomsen, F. Bertram, T. Riemann, J. Christen, K. Hiramatsu, T. Shibata and N. Sawaki: Appl. Phys. Lett. **74** (1999) 3320.
7) *User's Guide* (MARC Analyses Research Corporation, Palo Alto, 1996).
8) C. Kisielowski, J. Krüeger, S. Ruvimov, T. Suski, J. W. Ager, E. Jones, Z. Lilienthal-Weber, M. Rubin, E. K. Weber, M. D. Bremser and R. F. Davis: Phys. Rev. B **54** (1996) 17745.
9) Q. K. K. Liu, N. Moll, M. Scheffler and E. Pehlke: Phys. Rev. B **60** (1999) 17008.
10) Q. K. K. Liu, A. Hoffmann, H. Siegle, A. Kaschner, C. Thomsen, J. Christen and F. Bertram: Appl. Phys. Lett. **74** (1999) 3122.
11) S. Nakamura, M. Senoh, N. Iwasa, S. Nagahama, T. Yamada, T. Matsushita, H. Kiyoku and Y. Sugimoto: Jpn. J. Appl. Phys. **35** (1996) L217.